

Supplementary Information

Decoupled amphoteric water electrolysis and its integration with Mn-Zn battery for flexible utilization of renewables

Jianhang Huang,^a Yihua Xie,^a Lei Yan,^a Bingliang Wang,^a Taoyi Kong,^a Xiaoli Dong^{a*},
Yonggang Wang^{a*} and Yongyao Xia^{a,b}

^aDepartment of Chemistry and Shanghai Key Laboratory of Molecular Catalysis and Innovative Materials, Institute of New Energy, iChEM (Collaborative Innovation Center of Chemistry for Energy Materials), Fudan University, Shanghai 200433, China.

^bKey Laboratory of the Ministry of Education for Advanced Catalysis Materials, Department of Chemistry, Zhejiang Normal University, Jinhua 321004, China.

Experimental Procedures

Material preparation. All materials were used as received: Manganese(II) sulfate monohydrate ($\text{MnSO}_4 \cdot \text{H}_2\text{O}$, AR), sulfuric acid (H_2SO_4 , AR), potassium hydroxide (KOH, 85%) and zinc oxide (ZnO, AR). Above reagents were brought from Sinopharm Chemical Reagent Co., Ltd; Bipolar membrane was brought from Huamo Tech. Co., Ltd; Carbon felt (thickness of 5 mm) was brought from Dalian Longtian Tech. Co., Ltd.

Characterization. Purity of produced hydrogen is investigated using differential electrochemical mass spectrometry (DEMS) analysis. In detail, A quadrupole mass spectrometer (LingLu QAS 100) was connected to the HER cell for DEMS measurements. The electrolysis process was performed by a Land BT2000 battery test system with an applied current of 1 mA cm^{-2} . The mass spectrometer is connected to the HER cell, which has two tubes as the purge/carrier gas inlet and outlet as well as the capillary column to DEMS. Pure Ar gas was used as the purge gas and the carrier gas during the test. Before the online detection, this device was purified with pure Ar for 60 min at a flow rate of 2 mL min^{-1} . After that, the system was purged with a typical flow rate of 2 mL min^{-1} through the reaction period. The gas generated from the cell was carried to the DEMS for analysis. The hydrogen is obtained by charging the HER cell that consists of a commercialized Pt coated Ti-mesh electrode (1 cm^2) as negative electrode, carbon felt (1 cm^2 , thickness of 5 mm) as positive electrode and electrolyte of $1 \text{ M MnSO}_4 + 1 \text{ M H}_2\text{SO}_4$. And the HER cell is charged at 1 mA cm^{-2} for 24 minutes.

The volume of produced hydrogen is measured using a typical drainage method. The HER cell consists of a commercialized Pt coated Ti-mesh electrode (1 cm^2) as negative electrode, carbon felt (1 cm^2 , thickness of 5 mm) as positive electrode and $1 \text{ M MnSO}_4 + 1 \text{ M H}_2\text{SO}_4$ electrolyte. And the HER cell is charged at 100 mA cm^{-2} for different times to obtain different volume of hydrogen.

Electrochemical measurements. Electrochemical measurements were conducted on an electrochemical workstation (BioLogic VSP-300). Commercial Pt-coated Ti-mesh (Pt electrode) electrode and $\text{RuO}_2/\text{IrO}_2$ -coated Ti-mesh electrode ($\text{RuO}_2/\text{IrO}_2$ electrode) serves as HER and OER electrode, respectively, to demonstrate the conception of decoupled amphoteric water electrolysis, carbon felt (5 mm thickness) is used for redox of $\text{MnO}_2/\text{Mn}^{2+}$. Geometric area of all electrodes mentioned above is 1 cm^2 . For acidic and alkaline electrolyte, Ag/AgCl and Hg/HgO is used as reference electrode, respectively. Note that the potential of working electrode vs. Hg/HgO is converted to vs. Ag/AgCl for comparative purposes, and $\text{Potential}_{\text{vs. Hg/HgO}} - 0.107 = \text{Potential}_{\text{vs. Ag/AgCl}}$ (**Figure 1b, 4b** and four-points probe measurement). Two-electrode configuration of decoupled amphoteric water electrolysis is given in **Figure S3a** to obtain LSV curves in **Figure 2a,b** and **S4**. Three-electrode configuration of decoupled amphoteric water electrolyser is given in **Figure S3b** to obtain potential curves in **Figure 2c, 4b, S9, S10** and **S16**. The membrane voltage is obtained by four-points configuration using the amphoteric water electrolyser (**Figure S12**). The area of bipolar membrane used in all above configurations is 2 cm^2 .

Supplementary Figures

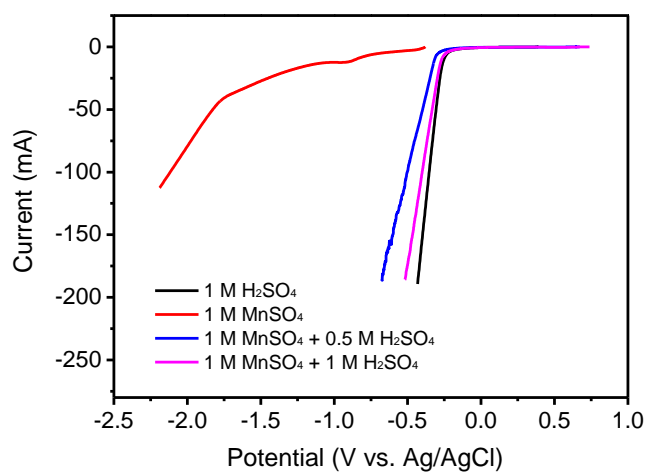


Figure S1. Influence of MnSO₄ on the HER process. LSV curves of HER process on Pt electrode in electrolyte with various concentration of MnSO₄ and H₂SO₄. In 1 M MnSO₄ electrolyte without H₂SO₄ (red curve), reduction of Mn²⁺ (reduction peak at -0.9 V vs. Ag/AgCl) is dominant compared with HER. With increase of H₂SO₄ concentration, the HER kinetics is much improved and HER process is dominated. There is only slight influence of manganese species on HER when H₂SO₄ concentration reaches 1 M. Scan rate: 5 mV s⁻¹.

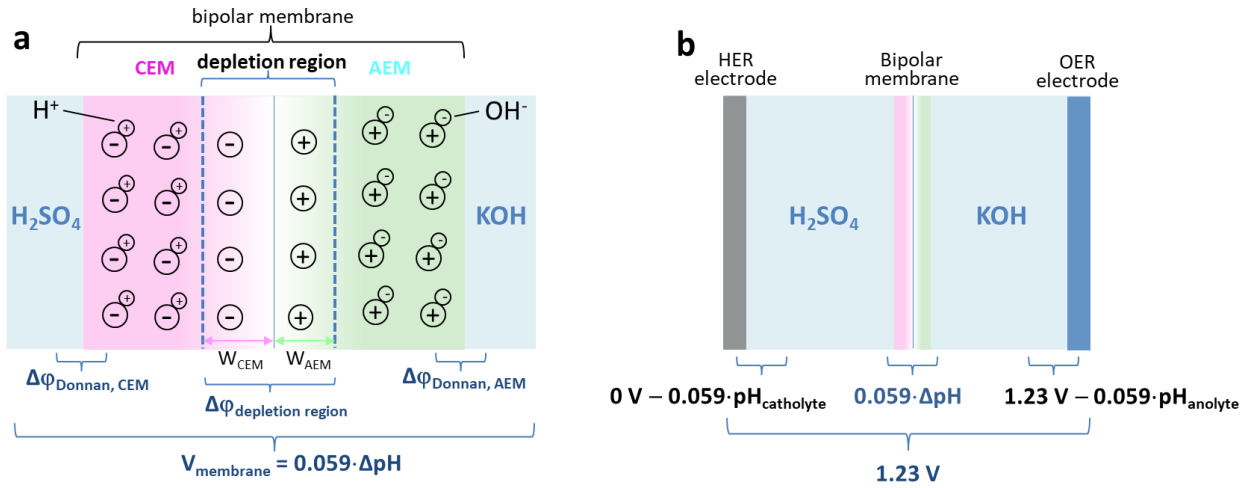


Figure S2. Illustration of membrane voltage in amphoteric electrolysis when CEM side of bipolar membrane faces acidic electrolyte and AEM side faces alkaline electrolyte (denoted as orientation-1). (a) Illustration of the CEM/AEM junction of bipolar membrane with orientation-1 at equilibrium state. (b) Analysis of the thermodynamic voltage required for amphoteric water electrolysis with orientation-1. It can be seen that the thermodynamic voltage required for water electrolysis with amphoteric electrolyte is equal to single electrolyte (1.23 V).

Illustration of electric field of BPM with orientation-1 at equilibrium state is shown in Figure S2a. The electrochemical behavior of CEM/AEM junction of BPM has been modeled and characterized in previous works.¹⁻³ A depletion region formed at the CEM/AEM conjunction results to potential difference (membrane voltage V_{membrane}). In detail, when the amphoteric electrolyte is separated by BPM, the mobile protons and hydroxide ions in the CEM and AEM respectively will neutralize to form H_2O in the conjunction of CEM/AEM, leading to the formation of depletion layer (Figure S2a). In the depletion layer, the fixed anions remaining in the CEM create an electric field (W_{CEM}) which electrostatically opposes the diffusion of additional protons from the CEM to the CEM/AEM junction. Likewise, there is another electric field (W_{AEM}) created at AEM side in depletion layer. The potential difference across the depletion region caused by W_{CEM} and W_{AEM} is denoted as $\Delta\phi_{\text{depletion region}}$. In addition, there is Donnan potential differences at membrane/electrolyte interfaces, which is denoted as $\Delta\phi_{\text{Donnan, CEM}}$ and $\Delta\phi_{\text{Donnan, AEM}}$ for the Donnan potential differences at CEM/electrolyte interface and AEM/electrolyte interface, respectively. As a result, the total potential difference across the membrane (membrane voltage) is denoted as $V_{\text{membrane}} = \Delta\phi_{\text{depletion region}} + \Delta\phi_{\text{Donnan, CEM}} + \Delta\phi_{\text{Donnan, AEM}}$, which can be determined by follow question:

$$V_{\text{membrane}} = \frac{RT}{F} \ln \left(\frac{[\text{H}^+]_{\text{catholyte}}}{[\text{H}^+]_{\text{anolyte}}} \right) \approx 0.059 \cdot \Delta\text{pH} \quad (\text{equation 1})$$

Where R is the universal gas constant ($8.31 \text{ J mol}^{-1} \text{ K}^{-1}$), T is the absolute temperature (K), F is the Faraday constant (96485 C mol^{-1}), $[\text{H}^+]$ is the proton concentration of catholyte and anolyte (M), and ΔpH is the pH difference over the bipolar membrane ($\text{pH}_{\text{anolyte}} - \text{pH}_{\text{catholyte}}$). Figure S2b shows the illustration of thermodynamic voltage required for water electrolysis with bipolar membrane in amphoteric electrolyte. The thermodynamic potential for HER in acidic electrolyte is $0 \text{ V} - 0.059 \cdot \text{pH}_{\text{catholyte}}$, and the potential for OER in alkaline electrolyte is $1.23 \text{ V} - 0.059 \cdot \text{pH}_{\text{anolyte}}$. If only take consideration of potential for HER and OER in amphoteric electrolyte, it requires $(1.23 \text{ V} - 0.059 \cdot \text{pH}_{\text{anolyte}}) - (0 \text{ V} - 0.059 \cdot \text{pH}_{\text{catholyte}}) = 1.23 - 0.059 \cdot \Delta\text{pH}$. But considering the bipolar membrane voltage of $0.059 \cdot \Delta\text{pH}$, the total thermodynamic voltage for amphoteric water electrolysis is 1.23 V, which is equal to that of single electrolyte. Above analysis indicates that amphoteric water electrolysis with bipolar membrane is able to accommodate the optimal pH conditions simultaneously for both HER and OER without changing the overall thermodynamics of water splitting.

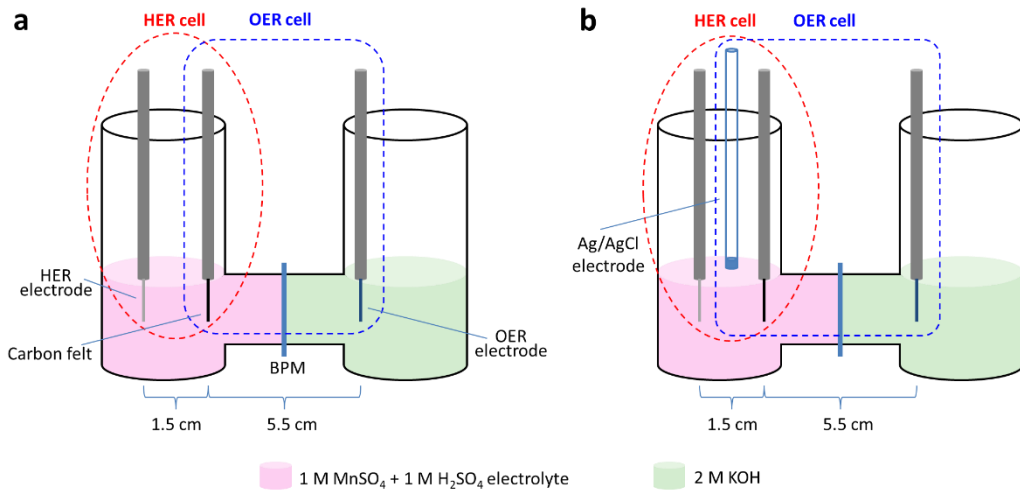
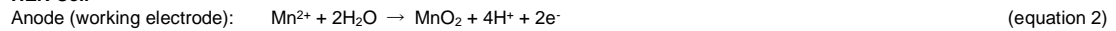
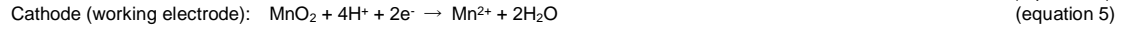


Figure S3. Configuration of proof-of-concept decoupled amphoteric water electrolyser. (a) Two-electrode configuration for decoupled HER and OER. The red LSV curve in **Figure 2a** is obtained with HER cell indicated by red dotted circle, in which working electrode is HER electrode, carbon felt is used as counter electrode and reference electrode. And the black LSV curve in **Figure 2a** is obtained by replacing the carbon felt with OER electrode in acidic electrolyte of 1 M H₂SO₄ without MnSO₄; The LSV curve in **Figure 2b** is obtained with OER cell indicated by blue dotted circle, in which working electrode is OER electrode, carbon felt with deposited MnO₂ is used as counter electrode and reference electrode. (b) Three-electrode configuration for decoupled HER and OER process. The potential curves for HER process in **Figure 2c** (left part) is obtained with HER cell indicated by red dotted circle, in which carbon felt is working electrode, HER electrode serves as counter electrode and Ag/AgCl serves as reference electrode. The HER cell is galvanostatic charged to 1 mAh cm⁻² at 100 mA cm⁻²; The potential curves for OER process in **Figure 2c** (right part) is obtained with OER cell indicated by blue dotted circle, in which carbon felt with deposited MnO₂ in HER process is working electrode, OER electrode serves as counter electrode and Ag/AgCl serves as reference electrode. The OER cell is galvanostatic discharged to -1.1 V at 10 mA cm⁻². The negative discharge platform of OER cell in **Figure 2c** indicates that the OER process need external bias.

HER Cell



OER Cell



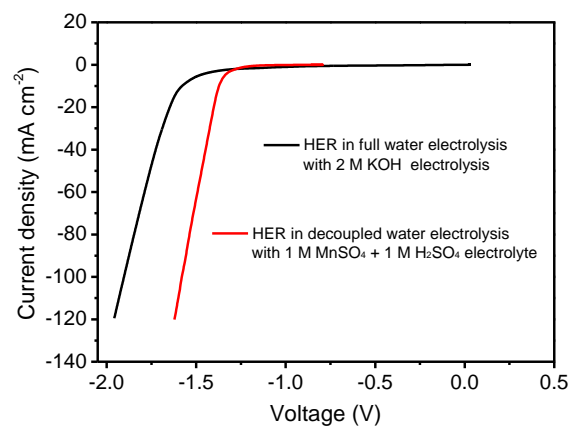


Figure S4. Comparison of LSV curves between decoupled water electrolysis and alkaline water electrolysis. Red curve: LSV of HER electrode in 1 M MnSO_4 + 1 M H_2SO_4 electrolyte, carbon felt as the counter and reference electrode. Black curve: LSV of HER electrode in 2 M KOH electrolyte, an OER electrode as counter and reference electrode. Scan rate: 5 mV s^{-1} . It requires -1.9 V and -1.58 V for conventional and decoupled water electrolysis to reach 100 mA cm^{-2} , shows 320 mV superiority of decoupled HER.

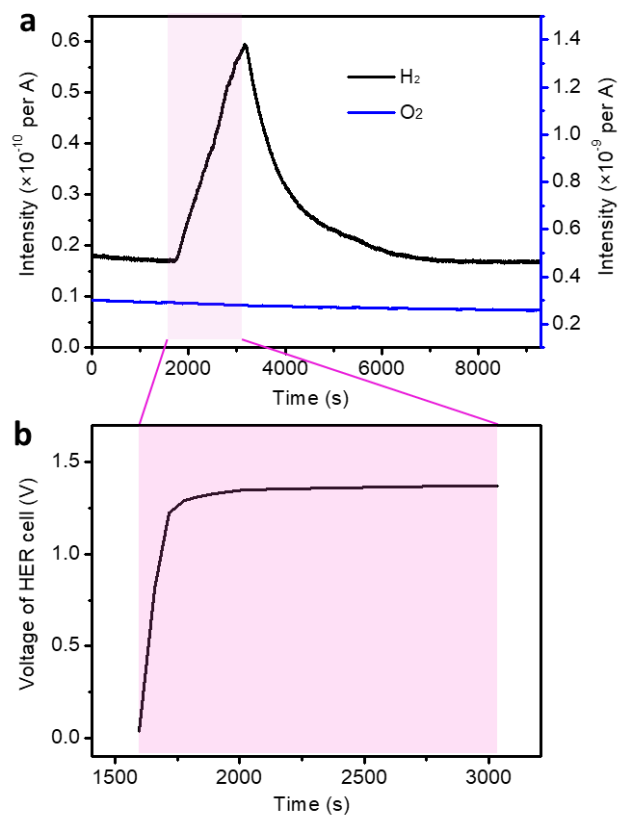


Figure S5. DEMS analysis of hydrogen purity. (a) High pure H₂ production demonstrated by the in situ DEMS analysis. (b) The corresponding charge curves (voltage vs. time) of the HER cell at an current density of 1 mA cm⁻².

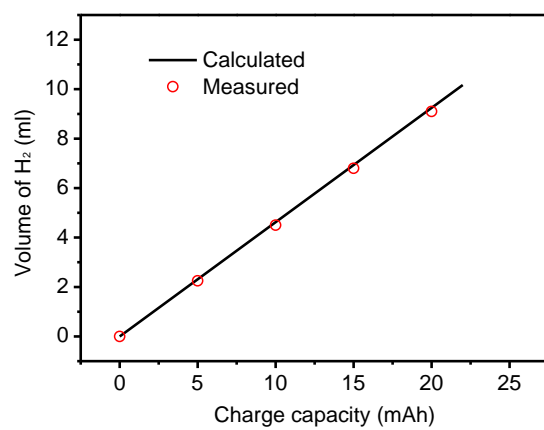


Figure S6. Comparison of the measured and theoretically calculated volume of H₂ during hydrogen production in HER cell at 100 mA cm⁻². Hydrogen volume is obtained using drainage method.

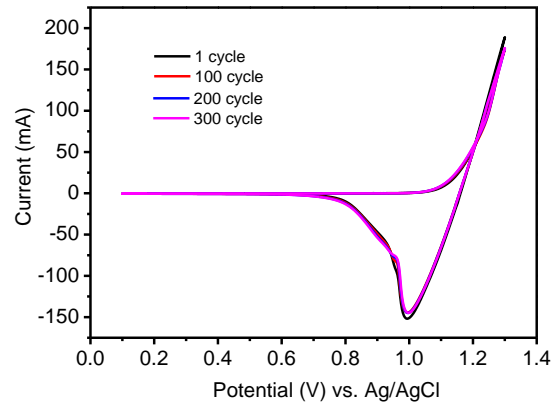


Figure S7. CV of carbon electrode in 1 M MnSO_4 + 1 M H_2SO_4 electrolyte with scan rate of 5 mV s^{-1} . Ag/AgCl serves as reference electrode, another carbon felt serves as counter electrode.

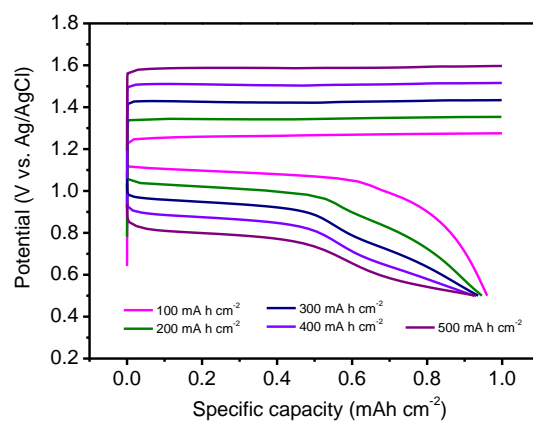


Figure S8. Charge/discharge curves of carbon felt in 1 M MnSO_4 + 1 M H_2SO_4 electrolyte with current density from 100 to 500 mA cm^{-2} . Ag/AgCl serves as reference electrode, another carbon felt serves as counter electrode. Working electrode carbon felt is galvanostatic charged to 1 mAh cm^{-2} and discharged to 0.5 V vs. Ag/AgCl at different current density from 100 to 500 mA cm^{-2} .

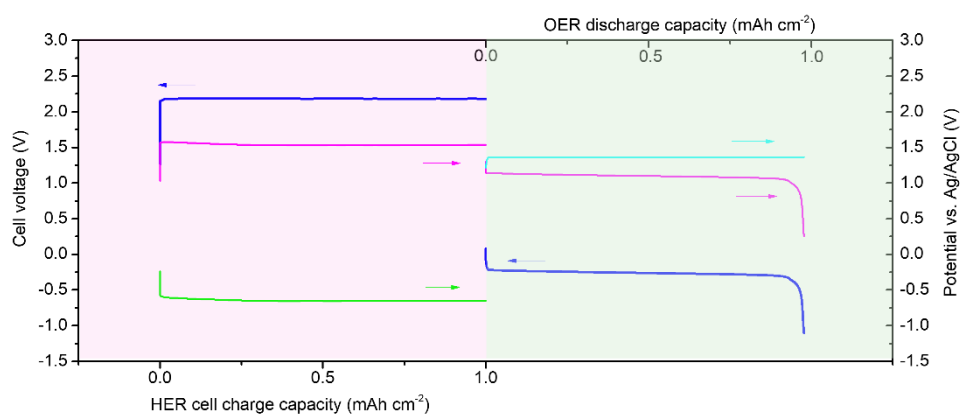


Figure S9. Potential curves of hydrogen production in HER cell (left part, 500 mA cm^{-2}) and oxygen production in OER cell (right part, 10 mA cm^{-2}) in decoupled amphoteric electrolyser. The configuration of the decoupled HER and OER cell is presented in **Figure S3b**. The charge curves of HER cell (left part) is obtained by charging the HER cell at 500 mA cm^{-2} to 1 mAh cm^{-2} . Carbon felt is working electrode, HER electrode serves as counter electrode and Ag/AgCl serves as reference electrode; The discharge curves of OER cell (right part) is obtained by discharging OER cell to -1.1 V at 10 mA cm^{-2} . Carbon felt with deposited MnO_2 in HER process is working electrode, OER electrode serves as counter electrode and Ag/AgCl serves as reference electrode. The negative discharge platform of OER cell indicates that the OER process need external bias.

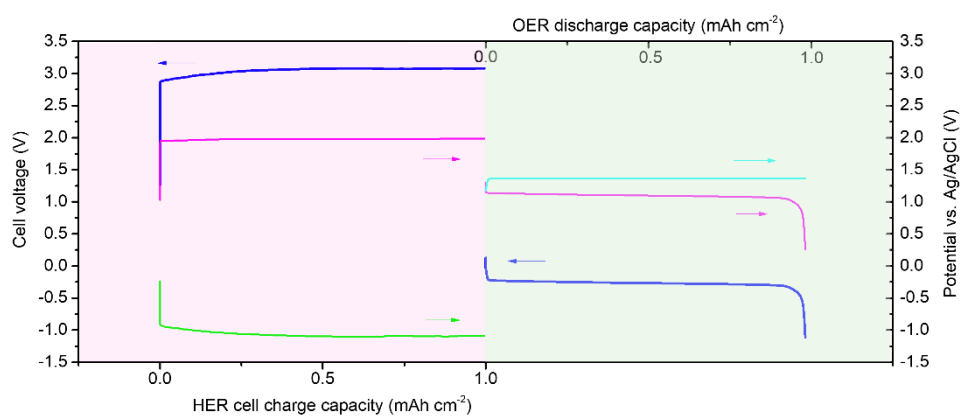


Figure S10. Potential curves of hydrogen production in HER cell (left part, 1000 mA cm^{-2}) and oxygen production in OER cell (right part, 10 mA cm^{-2}) in decoupled amphoteric electrolyser. The configuration of the decoupled HER and OER cell is presented in **Figure S3b**. The charge curves of HER cell (left part) is obtained by charging the HER cell at 1000 mA cm^{-2} to 1 mAh cm^{-2} . Carbon felt is working electrode, HER electrode serves as counter electrode and Ag/AgCl serves as reference electrode; The discharge curves of OER cell (right part) is obtained by discharging OER cell to -1.1 V at 10 mA cm^{-2} . Carbon felt with deposited MnO_2 in HER process is working electrode, OER electrode serves as counter electrode and Ag/AgCl serves as reference electrode. The negative discharge platform of OER cell indicates that the OER process need external bias.

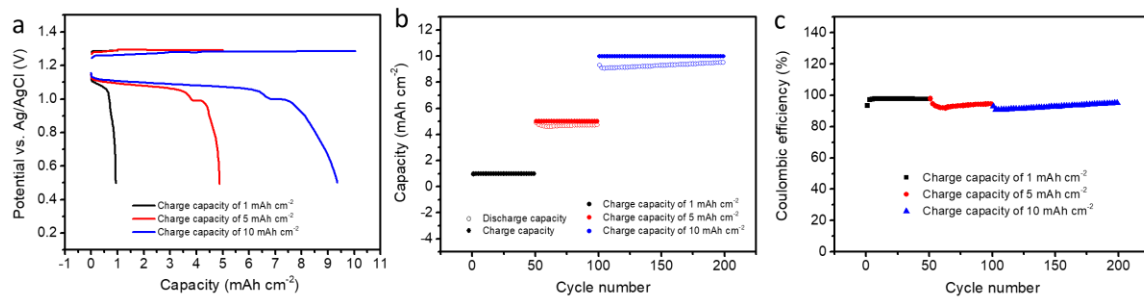


Figure S11. Cycle performance of MnO₂/Mn²⁺ redox chemistry with high deposition capacity in 1 M MnSO₄ + 1 M H₂SO₄ electrolyte. (a) Charge/discharge curves of MnO₂/Mn²⁺ under 1, 5 and 10 mAh cm⁻² deposition capacity. (b) Cycle performance of MnO₂/Mn²⁺ under 1, 5 and 10 mAh cm⁻² deposition capacity. (c) Coulombic efficiency of MnO₂/Mn²⁺ under 1, 5 and 10 mAh cm⁻² deposition capacity. Carbon felt is working electrode, Ag/AgCl serves as reference electrode, another carbon felt serves as counter electrode. Working electrode carbon felt is galvanostatic charged to different capacity and discharged to 0.5 V vs. Ag/AgCl. Charge/discharge current density is 100 mA cm⁻². The average Coulombic efficiency under 1, 5 and 10 mAh cm⁻² deposition capacity is 97.6%, 93.6% and 93%, respectively.

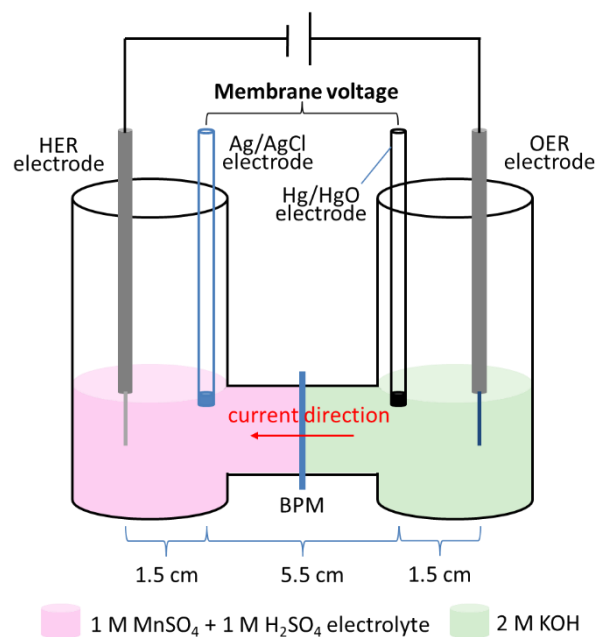


Figure S12. The configuration of four-points setup used to measure the potential drops (membrane voltage) across the bipolar membrane. HER and OER electrode are used to apply current across bipolar membrane. Ag/AgCl electrode and Hg/HgO electrode are used to obtain the potential drops across the bipolar membrane. The BPM, HER and OER electrode each had a geometric surface area of 2 cm^2 , 1 cm^2 and 1 cm^2 respectively.

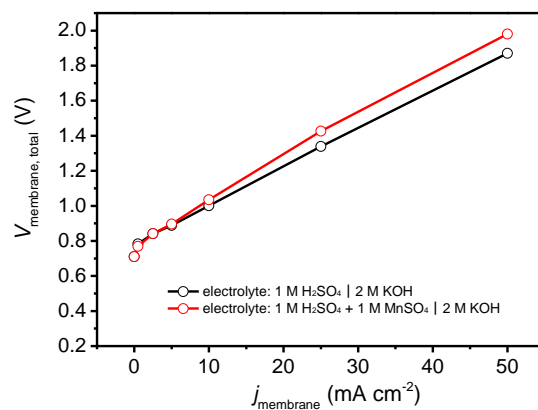


Figure S13. Influence of Mn^{2+} on the membrane voltage when the CEM side of BPM faces acidic electrolyte (orientation-1). The membrane voltages are obtained with four-points setup shown in **Figure S12**. Black curve: the acidic electrolyte is 1 M H_2SO_4 solution, and the alkaline electrolyte is 2 M KOH solution. Red curve: the acidic electrolyte is 1 M H_2SO_4 + 1 M MnSO_4 solution, and the alkaline electrolyte is 2 M KOH solution. The current density (j_{membrane}) across the BPM from OER electrode to HER electrode is on basis of membrane area (2 cm^2). It can be seen that there is no obvious influence of Mn^{2+} on membrane voltage when current density under 10 mA cm^{-2} .

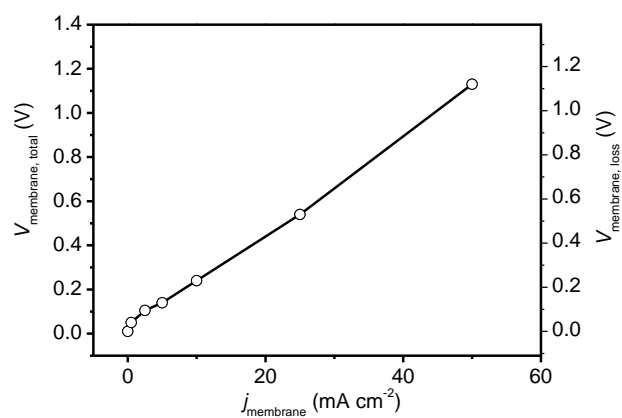


Figure S14. Bipolar membrane voltage and voltage loss when the CEM side of BPM faces alkaline electrolyte (orientation-2), which is obtained with four-points setup shown in **Figure S12**. The current density (j_{membrane}) across the BPM from OER electrode to HER electrode is on basis of membrane area (2 cm^2).

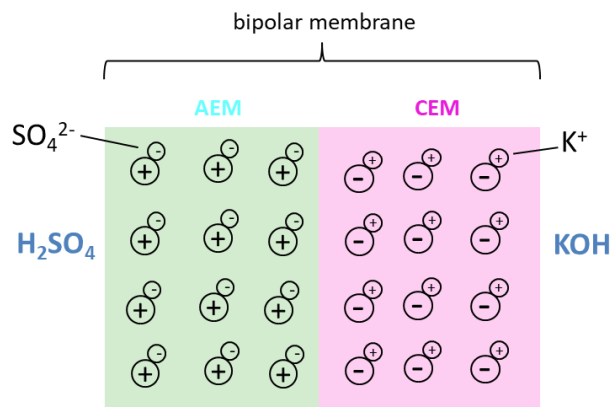


Figure S15. An illustration of the CEM/AEM conjunction when CEM side of bipolar membrane faces alkaline electrolyte and AEM side faces acidic electrolyte (orientation-2). Different from the orientation-1, the mobile ions in CEM and AEM is potassium ions and sulfate ions. Both of them are free ions, which can not form a depletion region. As a result, the membrane voltage at equilibrium state is zero.

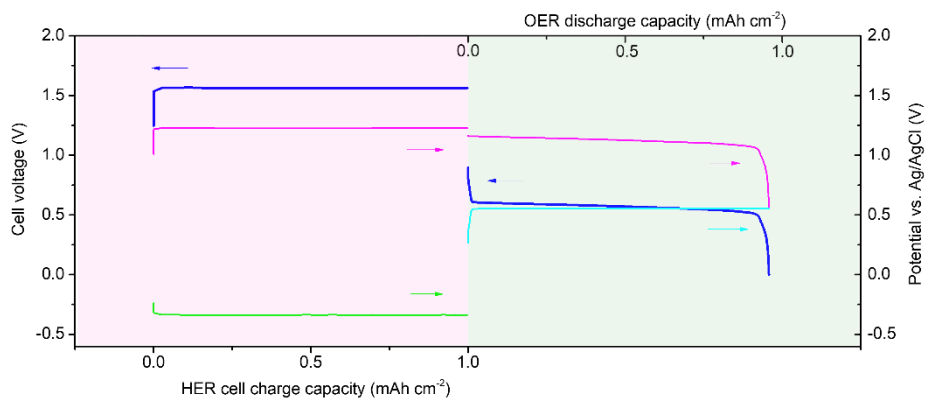


Figure S16. Potential curves of hydrogen production in HER cell (left part, 100 mA cm^{-2}) and oxygen production in OER cell (right part, 10 mA cm^{-2}) with membrane orientation-2 in decoupled amphoteric electrolyser. The configuration of the decoupled HER and OER cell is presented in **Figure S3b**. The charge curves of HER cell (left part) is obtained by charging the HER cell at 100 mA cm^{-2} to 1 mAh cm^{-2} . Carbon felt is working electrode, HER electrode serves as counter electrode and Ag/AgCl serves as reference electrode; The discharge curves of OER cell (right part) is obtained by discharging OER cell to 0 V at 10 mA cm^{-2} . Carbon felt with deposited MnO_2 in HER process is working electrode, OER electrode serves as counter electrode and Ag/AgCl serves as reference electrode.

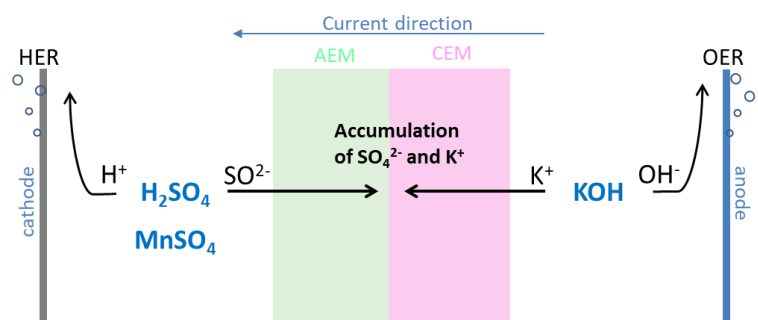


Figure S17. Working principle of BPM during water electrolysis when the CEM side of BPM faces alkaline electrolyte (orientation-2).

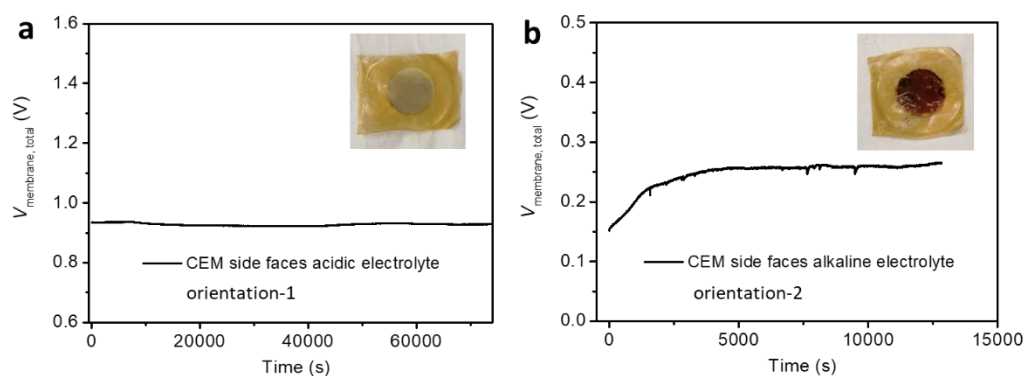


Figure S18. Development of membrane voltage as a function of time with (a) orientation-1 (CEM side of BPM faces acidic electrolyte) and (b) orientation-2 (CEM side of BPM faces alkaline electrolyte). The current density across the BPM from OER electrode to HER electrode is maintained at 5 mA cm^{-2} based on membrane area. The BPM, HER and electrode each had a geometric surface area of 2 cm^2 , 1 cm^2 and 1 cm^2 respectively. Inset: images of BPM after test. It can be seen that the amphoteric water electrolysis with orientation-1 is stable and sustainable, the membrane after long-time operating is clean and intact. On the contrary, amphoteric water electrolysis with orientation-2 is unsustainable, the membrane is damaged after several hours' electrolysis.

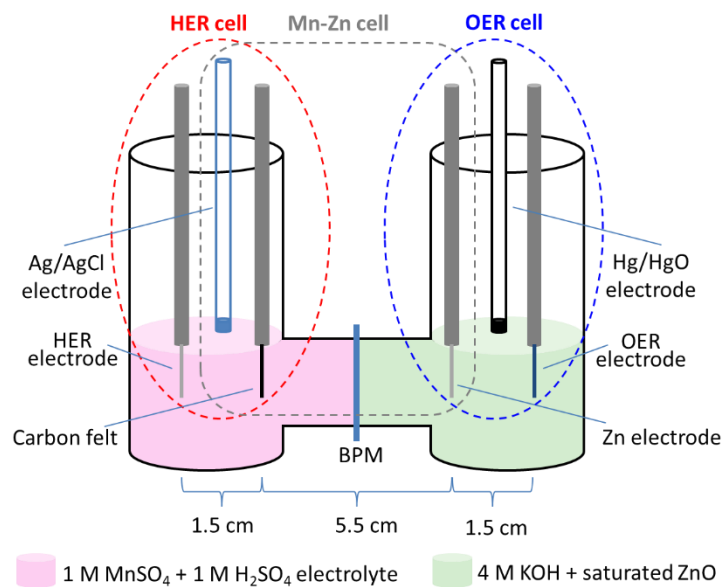


Figure S19. The configuration of integration system of decoupled amphoteric electrolyser and Mn-Zn battery. HER electrode and manganese electrode (carbon felt) in 1 M H₂SO₄ + 1 M MnSO₄ electrolyte form HER cell, in which manganese electrode, HER electrode and Ag/AgCl serves as working electrode, counter electrode and reference electrode, respectively; OER electrode and zinc electrode in 4 M KOH + saturated ZnO electrolyte form OER cell, in which OER electrode, zinc electrode and Hg/HgO serves as working electrode, counter electrode and reference electrode, respectively; Manganese electrode in 1 M H₂SO₄ + 1 M MnSO₄ electrolyte and zinc electrode in 4 M KOH + saturated ZnO electrolyte form Mn-Zn cell, in which manganese electrode, zinc electrode and Ag/AgCl serves as working electrode, counter electrode and reference electrode, respectively. BPM with orientation-1 is used to separate amphoteric electrolyte. The geometric surface area of BPM and electrode (including HER electrode, OER electrode, manganese electrode and zinc electrode) is 2 cm² and 1 cm², respectively.

Table S1 Comparison of energy efficiency of different systems

	Conventional water electrolysis	Decoupled system (two processes)	Integrated system (three processes)
Energy efficiency of decoupled HER process	--	80%	80%
Energy efficiency of decoupled OER process	--	0	0
Total efficiency	68%	70%	62%

The energy efficiencies of the conventional water electrolysis and decoupled water electrolysis (two or three processes) are estimated as follows:

$$\eta = E_{\text{hydrogen}}/E_{\text{water electrolysis}} \quad (\text{equation 7})$$

where η is the energy efficiency of water electrolysis; E_{hydrogen} is the heat released from combustion of hydrogen (the product of combustion is water vapor), which is derived from water electrolysis; and $E_{\text{water electrolysis}}$ is the energy consumed during water electrolysis. E_{hydrogen} is a constant value of 242 kJ mol⁻¹, which is equal to 67.2 Wh mol⁻¹. And the $E_{\text{water electrolysis}}$ can be calculated by follow equation:

$$E_{\text{water electrolysis}} = Ult = UQ \quad (\text{equation 8})$$

where U is the input voltage, I is the current density, t is time of duration, and Q is consumed quantity of electric charge. According to equation 8, when assuming Faraday efficiency is 100%, it requires 2 mol electrons to produce 1 mol hydrogen. And it needs 2 mol × 96485 C mol⁻¹ = 186970 C quantity of electric charge (96485 C mol⁻¹ is faraday constant), which is equal to 53.6 Ah. Finally, the energy efficiency of water electrolysis to produce 1 mol hydrogen is $\eta = 67.2/(U \times 53.6)$.

For the conventional acidic electrolysis, 1.84 V is required to reach 100 mA cm⁻² current density (which is estimated from LSV in **Figure 2a**), and $E_{\text{water electrolysis}} = 1.84 \times 53.6 = 98.6$ Wh. And $\eta = 67.2/98.6 = 68\%$, which is consistent with previous works^{4,5}.

The decoupled system has two processes of HER and OER (shown in **Figure 1a, 2c** in main text). HER process requires 1.56 V to reach 100 mA cm⁻² current density, and $\eta = 67.2/(1.56 \times 53.6) = 80\%$. OER process requires 0.24 V to produce oxygen, but the efficiency is zero due to the fact that there is no hydrogen is produced. And the total efficiency is $\eta = 67.2/((1.56 + 0.24) \times 53.6) = 70\%$.

The integration system has three processes of HER, OER and discharge of Mn-Zn cell (shown as **Figure 4** in main text). Herein, HER process requires 1.56 V to reach 100 mA cm⁻² current density, and $\eta = 67.2/(1.56 \times 53.6) = 80\%$. And OER process requires 2.15 V, but no hydrogen produced. However, there is energy that is stored in Mn-Zn cell, whose operating voltage is 1.7 V. Accordingly, the total efficiency of the integration system is $\eta = 67.2/((1.56 + 2.15 - 1.7) \times 53.6) = 62\%$.

According to above estimation, Table S1 summarized the energy efficiency for comparison. With the decoupled strategy, HER and OER can be divided completely, which makes it possible to reapportion energy consumption for HER and OER. The energy efficiency could be obviously improved from 68% to 80% for the HER process compared with conventional water electrolysis. Furthermore, HER and OER process can operate at different current densities in decoupled strategy, the low current density for OER is helpful to decrease polarization and improve energy efficiency of water electrolysis. The comparison indicated that the decoupled systems can not only ensure the high efficiency, but also show excellent flexibility to accommodate renewables, which can make full advantages of the intermittent renewables.

References

1. M. Unlu, J. F. Zhou and P. A. Kohl, *Journal of Physical Chemistry C*, 2009, **113**, 11416-11423.
2. K. Sun, R. Liu, Y. Chen, E. Verlage, N. S. Lewis and C. Xiang, *Advanced Energy Materials*, 2016, **6**, 1600379.
3. R. Pärnamäe, S. Mareev, V. Nikonenko, S. Melnikov, N. Sheldeshov, V. Zabolotskii, H. V. M. Hamelers and M. Tedesco, *Journal of Membrane Science*, 2021, **617**, 118538.
4. J. A. Turner, *Science*, 2004, **305**, 972-974.
5. S. E. Hosseini and M. A. Wahid, *Renewable and Sustainable Energy Reviews*, 2016, **57**, 850-866.